ESC European Society of Cardiology

European Heart Journal - Cardiovascular Imaging (2023) **00**, 1–9
https://doi.org/10.1093/ehjci/jead213

ORIGINAL PAPER

Three-dimensional echocardiographic evaluation of longitudinal and non-longitudinal components of right ventricular contraction: results from the World Alliance of Societies of Echocardiography study

Juan I. Cotella [1]*, Attila Kovacs[2], Karima Addetia[1], Alexandra Fabian[2], Federico M. Asch[3], and Roberto M. Lang[1] on behalf of the WASE Investigators†

[1]University of Chicago, Chicago, Illinois, USA; [2]Heart and Vascular Center, Semmelweis University, Budapest, Hungary; and [3]MedStar Health Research Institute, Washington, DC, USA

Received 7 June 2023; accepted 15 August 2023; online publish-ahead-of-print 21 August 2023

Aims Right ventricular (RV) functional assessment is mainly limited to its longitudinal contraction. Dedicated three-dimensional echocardiography (3DE) software enabled the separate assessment of the non-longitudinal components of RV ejection fraction (EF). The aims of this study were (i) to establish normal values for RV 3D-derived longitudinal, radial, and anteroposterior EF (LEF, REF, and AEF, respectively) and their relative contributions to global RVEF, (ii) to calculate 3D RV strain normal values, and (iii) to determine sex-, age-, and race-related differences in these parameters in a large group of normal subjects (WASE study).

Methods and results 3DE RV wide-angle datasets from 1043 prospectively enrolled healthy adult subjects were analysed to generate a 3D mesh model of the RV cavity (TomTec). Dedicated software (ReVISION) was used to analyse RV motion along the three main anatomical planes. The EF values corresponding to each plane were identified as LEF, REF, and AEF. Relative contributions were determined by dividing each EF component by the global RVEF. RV strain analysis included longitudinal, circumferential, and global area strains (GLS, GCS, and GAS, respectively). Results were categorized by sex, age (18–40, 41–65, and >65

* Corresponding author. E-mail: juanicotella@gmail.com; jcotella@bsd.uchicago.edu
† WASE Investigators.
Argentina: Aldo D. Prado, Centro Privado de Cardiologia, Tucumán, Argentina; Eduardo Filipini, Universidad Nacional de la Plata, Buenos Aires, Argentina; Ricardo E. Ronderos, Instituto Cardiovascular de Buenos Aires, Buenos Aires, Argentina.
Australia: Agatha Kwon and Samantha Hoschke-Edwards, Heart Care Partners, Queensland, Australia; Gregory M. Scalia, Genesis Care, Brisbane, Australia.
Brazil: Tania Regina Afonso and Ana Clara Tude Rodridugues, Albert Einstein Hospital, Sao Paulo, Brazil.
Canada: Babitha Thampinathan, Maala Sooriyakanthan, and Wendy Tsang, Toronto General Hospital, University of Toronto, Canada.
China: Mei Zhang, Yingbin Wang, and Yu Zhang, Qilu Hospital of Shandong University, Jinan, China; Tiangang Zhu and Zhilong Wang, Peking University People's Hospital, Beijing, China; Lixue Yin and Shuang Li, Sichuan Provincial People's Hospital, Sichuan, China.
India: R. Alagesan, Madras Medical College, Chennai, India; S. Balasubramanian, Madurai Medical College, Madurai, India; R.V.A. Ananth and Vivekanandan Amuthan, Jeyalakshmi Heart Center, Madurai, India; Manish Bansal, Medanta Heart Institute, Medanta, Haryana, India; Ravi R. Kasliwal, Medanta Heart Institute, Gurgaon, Haryana, India.
Iran: Azin Alizadehasl, Rajaie Cardiovascular Medical Center, IUMS, Tehran, Iran; Anita Sadeghpour, Rajaie Cardiovascular Medical and Research Center, Tehran, Iran.
Italy: Luigi Badano and Denisa Muraru, University of Milano-Bicocca, and Istituto Auxologico Italiano, IRCCS, Milan, Italy; Eduardo Bossone, Davide Di Vece, Rodolfo Citro and Michele Bellino, University of Salerno, Salerno, Italy
Japan: Tomoko Nakao, Takayuki Kawata, Megumi Hirokawa, Naoko Sawada and Masao Daimon, The University of Tokyo, Tokyo, Japan; Yousuke Nabeshima and Masaki Takeuchi, University of Occupational and Environmental Health, Kitakyushu, Japan
Republic of Korea: Hye Rim Yun, Seung Woo Park and Ji-won Hwang, Samsung Medical Center, Seoul, Republic of Korea
Mexico: Pedro Gutierrez Fajardo, Hospitales Mac Bernardette, Guadalajara, Mexico
Nigeria: Kofo O. Ogunyankin, First Cardiology Consultants Hospital, Lagos, Nigeria
Phillipines: Edwin S. Tucay, Philippine Heart Center, Quezon City, Philippines
United Kingdom: Mark J. Monaghan, King's College Hospital, London, United Kingdom
United States: James N. Kirkpatrick, University of Washington, Seattle, WA; Tatsuya Miyoshi, MedStar Health Research Institute, Washington, DC

years), and race. Absolute REF, AEF, LEF, and global RVEF were higher in women than in men ($P < 0.001$). With aging, both sexes exhibited a decline in all components of longitudinal shortening ($P < 0.001$), which was partially compensated in elderly women by an increase in radial contraction. Black subjects showed lower RVEF and GAS values compared with white and Asian subjects of the same sex ($P < 0.001$), and black men showed significantly higher RV radial but lower longitudinal contributions to global RVEF compared with Asian and white men.

Conclusion 3DE evaluation of the non-longitudinal components of RV contraction provides additional information regarding RV physiology, including sex-, age-, and race-related differences in RV contraction patterns that may prove useful in disease states involving the right ventricle.

Graphical Abstract

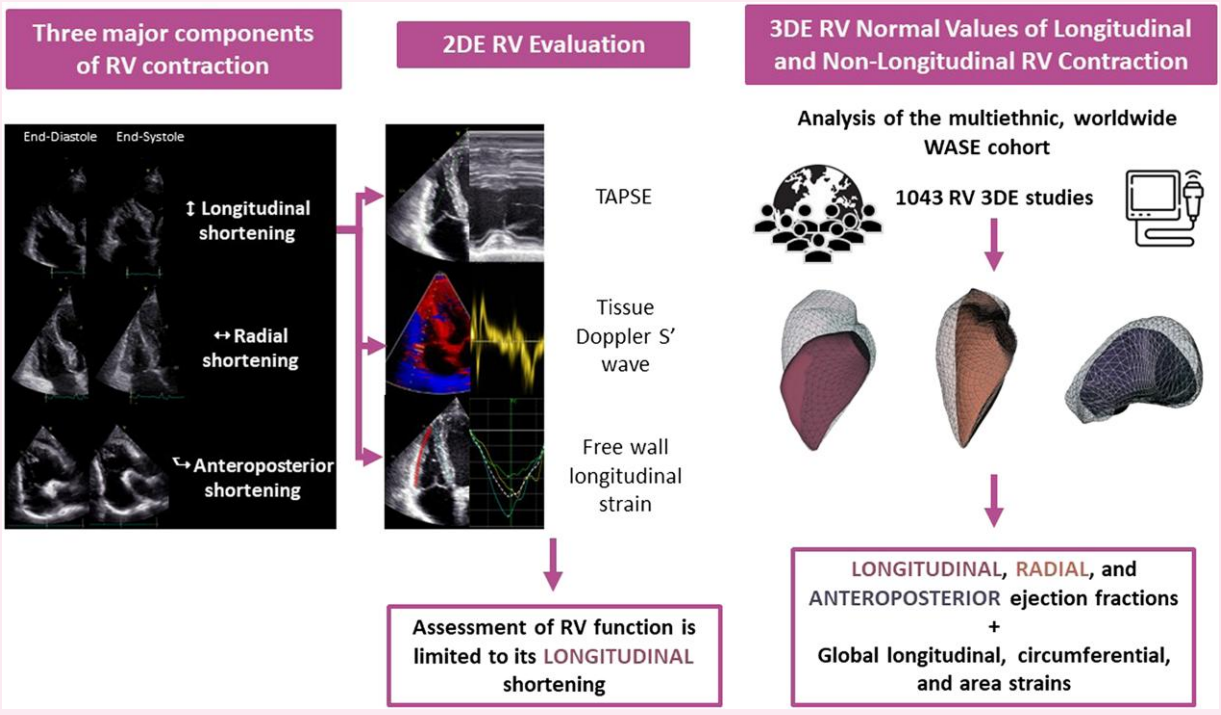

Pathophysiological advantages of 3D RV decomposition into longitudinal and non-longitudinal contractile components.

Keywords right ventricle • three-dimensional echocardiography • non-longitudinal

Introduction

Right ventricular (RV) function has a prognostic role in several cardiovascular diseases.[1–4] In clinical practice, RV evaluation is predominantly performed using transthoracic echocardiography (TTE) and is based on the interpretation of two-dimensional (2D) measurements such as follows: basal and mid-ventricular diameters, fractional area change (FAC), tricuspid annular plane systolic excursion (TAPSE), tissue Doppler tricuspid annular velocity, and RV free-wall strain (RV FWS).

However, the right ventricle has a complex anatomy and an intricate contraction pattern. Due to the different orientation of its subepicardial (circumferential) and subendocardial (longitudinal) myocardial fibres,[5] RV contraction occurs along the longitudinal, radial, and anteroposterior directions. As a result, simple 2D echocardiographic (2DE) techniques might be inadequate to accurately evaluate RV performance, as they provide information limited to the in-plane components of motion.

Three-dimensional echocardiography (3DE) allows the evaluation of the entire right ventricle from a single acquisition. Through the generation, manipulation, and decomposition of 3DE dynamic rendering models, recently developed software has enabled the separate assessment of the longitudinal and non-longitudinal components of RV function and the quantification of their relative contributions to global RV performance.[6] However, little is known about what these components look like in the normal population, and therefore, there is no reference basis to detect abnormalities.

Accordingly, the aims of this study were as follows: (i) to establish normal values for longitudinal, radial, and anteroposterior components of RV contraction and determine their relative contributions to global RV performance in a large group of normal subjects, (ii) to calculate 3D RV strain normal values, and (iii) to examine sex-, age-, and race-related differences in these values. To achieve these goals, we used the World Alliance Societies of Echocardiography (WASE) study population, which represents the largest collection of normal TTE images.

Methods

Study design and population

The WASE study rationale was described elsewhere.[7,8] A comprehensive 2D and 3D TTE examination was performed using commercial ultrasound imaging systems (GE, Philips, and Siemens). Image acquisition followed a standard protocol established by ASE/EACVI guidelines and data analysed by WASE core laboratories (University of Chicago and MedStar Health Research Institute).[9]

Image acquisition and analysis

Wide-angle 3DE RV datasets were acquired with the patient in the left decubitus position over 4–6 cardiac cycles during suspended respiration from the RV-focused view. Data were digitally stored and analysed offline using dedicated vendor-independent software (Image Arena; '4D RV-Function', TOMTEC, Unterschleissheim, Germany), previously validated against cardiac magnetic resonance (CMR).[9,10] 3DE datasets were deemed adequate for analysis if all walls were visible throughout the cardiac cycle and a minimum frame rate of 15 volumes/s was achieved.

Auto-segmentation technology with the help of manually identified landmarks allowed the 3D RV dataset to be displayed in both the long- and short-axis cut-planes with an initial endocardial border contour suggestion. End-diastole and end-systole were automatically identified as the time points at which the RV cavity was the largest and smallest, respectively. Afterwards, the user could manually adjust the proposed end-diastolic and end-systolic endocardial contours to optimize dynamic tracking throughout the cardiac cycle. Once this was completed, the program generated and rendered a 3D RV surface model.

Decomposition of the RV motion

Figure 1 shows a brief representation of the workflow used for the decomposition of RV contraction into its three major components.

First, the 3D RV models (formulated as a series of polygon meshes) were exported throughout the cardiac cycle from the TOMTEC software into ReVISION software (Right Ventrlcular Separate wall motlon quantificatiON; Argus Cognitive, Lebanon, New Hampshire).[6]

To standardize the orientation and decomposition of the RV contraction, the 3D RV models were aligned to a reference mesh by methodology described elsewhere[11] aiming to define three anatomically relevant, orthogonal axes of the right ventricle as follows: longitudinal, radial, and anteroposterior.

Initially, RV end-diastolic volume indexed (EDVi) to body surface area (BSA) and global RVEF were calculated. Once the relevant axes were defined, the wall motion of the RV model was decomposed in a vertex-based manner. This step transformed the original 3D polygon mesh model into several series of meshes, each corresponding to a decomposition type, allowing the isolation and independent assessment of the magnitude of longitudinal, radial, or anteroposterior motions.

By decomposing the model's motion along the predefined orthogonal axes, the software was capable to separately quantify RV volume changes along each direction using the signed tetrahedron method.[6] The corresponding EF value for each axis was defined as longitudinal, radial, and anteroposterior EF (LEF, REF, and AEF, respectively). The relative and individual contributions of LEF, REF, and AEF to the global RV performance were calculated as ratios, dividing each axis EF by the global RVEF (LEF/RVEF, REF/RVEF, and AEF/RVEF, respectively).

Importantly, the absolute volume change corresponds to the aggregated contribution of the three motion components. This composition is not additive, and consequently, the sum of the decomposed volume changes is not equal to the global RV volume change.[12]

Finally, 3D RV global longitudinal and circumferential strains (GLS, GCS) were calculated by the changes in predefined longitudinal and circumferential contour lengths referenced to the corresponding end-diastolic length. Briefly, to obtain 3D RV GLS, 45 longitudinally oriented contours were generated by connecting the apex and predefined vertices of the base through specific equidistant vertices at the middle section by fitting geodesic lines (the shortest path between two points on a curved surface). This method ensures that the longitudes are evenly distributed on the mesh surface. Ultimately, the quantification of the change in the length of each longitudinal contour throughout the cardiac cycle allowed the calculation of 3D RV GLS. For the calculation of 3D RV GCS, the pulmonary and tricuspid annular planes were excluded. Then, 15 circumferential contours were created by slicing horizontally the RV mesh model at equal distances along the longitudinal axis. After generating a set of circumferential contours, the change in their positions was quantified at later time instants to provide 3D RV GCS values.

Additionally, 3D RV GAS was defined as the percentage change in the endocardial area of the 3D models. *Figure 2* (*Graphical abstract*) illustrates the pathophysiological value of the 3D analysis of the multiple components of RV contraction.

Statistical analysis

All data are presented as mean ± SD. Group differences were evaluated using ANOVA and unpaired two-tailed Student's *t*-tests. Statistical significance was defined as $P < 0.05$. Normal ranges for each parameter were defined as upper and lower limits of normal (ULN and LLN, respectively) using 2.5th and 97.5th percentiles from the relevant group. This is in accordance

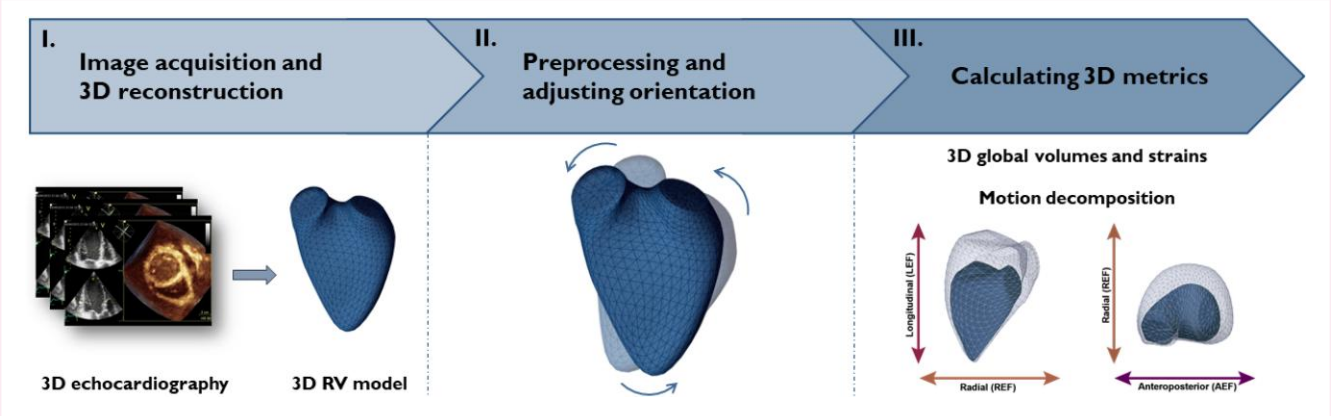

Figure 1 Schematic representation of the workflow used for the decomposition of RV contraction into its three major components.

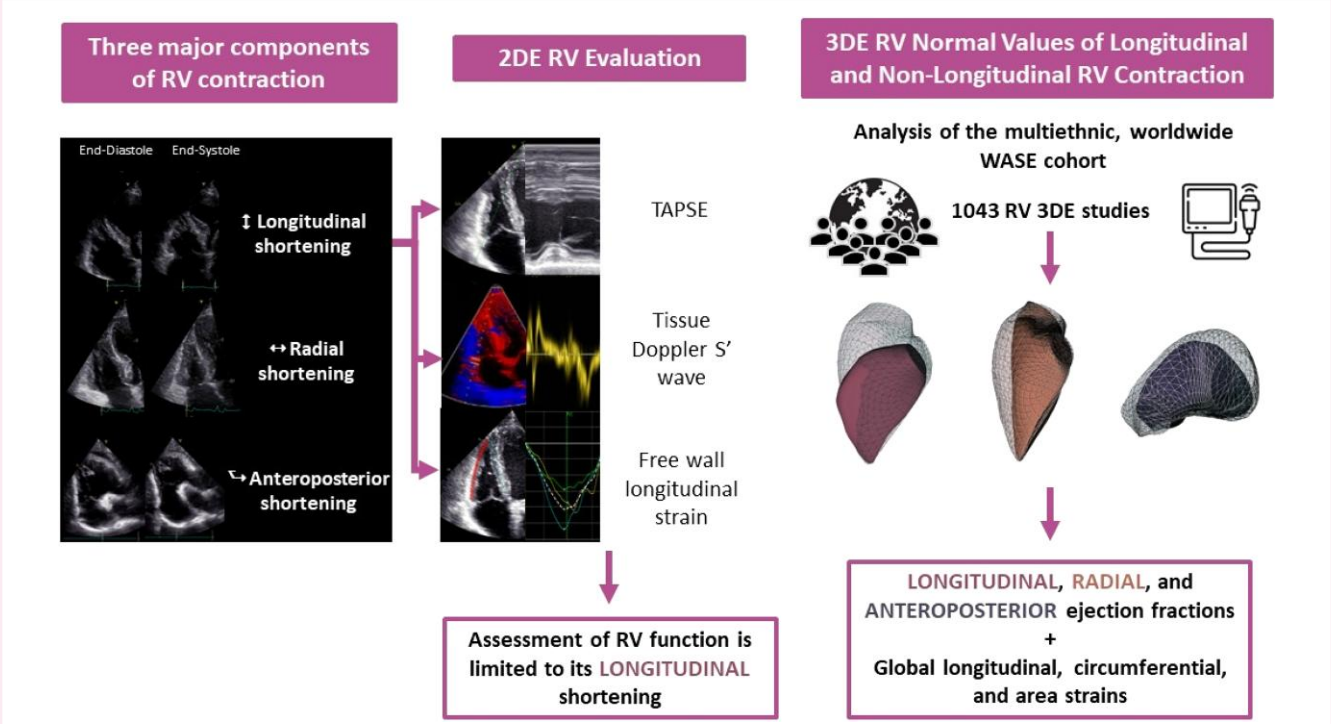

Figure 2 Pathophysiological advantages of 3D RV decomposition into longitudinal and non-longitudinal contractile components.

Table 1 Basic anthropometric and demographic data in the total study population and separately in men and women

	All subjects $n = 1043$	Men $n = 533$	Women $n = 510$	*P*-value
Age (years)	46.8 ± 16.6	46.2 ± 16.4	47.4 ± 16.8	0.245
Heart rate (bpm)	64.6 ± 10.5	63.5 ± 10.3	65.7 ± 10.5	**0.001**
Systolic blood pressure (mmHg)	121 ± 74	123 ± 12	118 ± 13	**0.001**
Diastolic blood pressure (mmHg)	74 ± 9	75 ± 8	72 ± 9	**0.001**
BSA (m^2)	1.78 ± 0.21	1.89 ± 0.19	1.66 ± 0.17	**<0.001**
Left ventricular function parameters				
LVEF (%)	61 ± 5	60 ± 5	62 ± 5	**0.000**
LV GLS	−21.2 ± 3.1	−20.7 ± 3.1	−21.8 ± 2.9	**0.000**
LV GCS	−31.5 ± 4.0	−31.0 ± 4.0	−32.1 ± 3.9	**0.000**
Race				
Asian	375 (36%)	206 (39%)	169 (33%)	0.064
Black	142 (14%)	69 (13%)	73 (14%)	0.519
White	488 (47%)	235 (44%)	253 (50%)	0.074
Other (mixed and other)	38 (4%)	23 (4%)	15 (3%)	0.236

Statistically significant *P*-values are shown in bold characters.
Y, years; bpm, beats per minute; BSA, body surface area; LVEF, left ventricular ejection fraction; LV GLS, left ventricular global longitudinal strain; LV GCS, left ventricular global circumferential strain.

with the definition of 'normal' as falling within 95% of the normal population, with the remaining 5% being distributed equally between the two tails, irrespective of whether the distribution is Gaussian. Pearson or Spearman correlation tests were applied, as appropriate. In addition, multivariable linear regression analyses were performed to identify independent associations with demographic, anthropometric, basic haemodynamic, and left ventricular (LV) functional parameters. The corresponding values of LV functional parameters were obtained from a prior WASE publication on

3D LV function and then matched to each patient included in our study. The details regarding the acquisition and analysis of 3D LV function were previously described.[13] To add race, we dichotomized our cohort accordingly, analysing white (yes/no), black (yes/no), and Asian (yes/no) races as separate variables in each model to avoid collinearity.

Results

Out of the initial cohort of 2262 subjects from the WASE study, 2007 had 3D RV datasets in the format suitable for measurement. Of these, 1043 (52%) had adequate image quality. Exclusion criteria were as follows: (i) low frame rates (<15 volumes/s), (ii) stitch artefact, (iii) excessive drop-out of the anterior RV free wall, and (iv) incomplete data capture with the lateral free wall or the RV apex being cut-off from the pyramidal volume. *Table 1* shows the basic anthropometric and demographic data of the study population. Most of the population was white (47%) followed by Asians (36%). Subjects were divided into six subgroups according to age and sex as follows: 18–40 years (234 men, 199 women), 41–65 years (194 men, 197 women), and >65 years (105 men, 114 women). Corresponding parameters of LV function were also included in this table. ULN and LLN for global and direction-specific RV functional parameters are reported in *Table 2*.

Table 3 shows the 3D RV morphological and functional parameters of the study population and separated by sex. RVEDVi was significantly higher in men ($P < 0.001$). Global RVEF and absolute REF, AEF, and LEF values were higher in women ($P < 0.001$). However, the relative contribution of each of the individual components to the global RVEF was similar in both sexes. While GLS and GAS were significantly higher in women, GCS showed no differences between sexes.

Table 4 shows the age-related differences in the components of 3D RV systolic function in both sexes. There were no significant differences in RVEDVi between age groups. Both sexes exhibited a decline in longitudinal shortening (i.e. LEF, LEF/RVEF, and GLS, $P < 0.001$) with increasing age. In women, this reduction in LEF/RVEF led to a lower global RVEF ($P < 0.001$), which was incompletely compensated by an increase in REF/RVEF.

BSA and RVEDVi were significantly smaller in Asian compared with black and white subjects (*Table 5*). Both black men and women showed lower RVEF, and GAS values compared with white and Asian subjects of the same sex ($P < 0.001$). Black men showed a distinctive RV mechanical pattern, consistent of significantly higher REF/RVEF and lower LEF/RVEF values, when compared with Asian and white men. White men showed higher LEF/RVEF than both black and Asian men ($P < 0.001$). These differences in RV contraction patterns across races were not significant in women.

Correlations between LEF, REF, and AEF and basic demographic, anthropometric, haemodynamic, and LV functional parameters are summarized in Supplementary data online, *Table S1*. 3DE-derived LVEF correlated weakly with 3D RVEF ($r = 0.161$, $P < 0.001$), LEF ($r = 0.112$, $P = 0.001$), and AEF ($r = 0.126$, $P < 0.001$). 3D LV GLS also correlated weakly with 3D RVEF ($r = -0.158$, $P < 0.001$), 3D RV GLS ($r = 0.166$, $P < 0.001$), and LEF ($r = -0.238$, $P < 0.001$). Results of multivariable analyses are shown in Supplementary data online, *Tables S2–S4*. Beyond age, sex, and LVEF, white and black races were independent predictors of LEF, whereas sex, LVEF, and white and black races were independent predictors of AEF.

Table 2 Upper and lower limits of normality for the novel RV parameters in men and women

	All subjects $n = 1043$	Men $n = 533$	Women $n = 510$
	LLN to ULN	LLN to ULN	LLN to ULN
RVEDVi (ml)	43.7 to 123.1	47.9 to 132.5	41.7 to 110.6
RVEF (%)	44.7 to 67.1	44.1 to 65.7	45.8 to 68.6
RV GCS	−13.4 to −31.3	−13.9 to −30.9	−12.8 to −31.6
RV GLS	−13.2 to −27.4	−13.4 to −26.9	−12.5 to −27.9
RV GAS	−28.4 to −48.9	−28.5 to −47.6	−28.4 to −49.6
REF (%)	15.3 to 42.7	15.0 to 41.8	15.7 to 43.1
REF/RVEF	0.30 to 0.73	0.29 to 0.73	0.30 to 0.73
AEF (%)	14.1 to 37.2	13.7 to 35.3	14.2 to 37.8
AEF/RVEF	0.28 to 0.61	0.28 to 0.60	0.28 to 0.61
LEF (%)	11.1 to 33.4	11.7 to 31.7	11.0 to 35.0
LEF/RVEF	0.22 to 0.56	0.23 to 0.55	0.22 to 0.57

Ml, millilitres; LLN, lower limit normal (2.5th percentile); ULN, upper limit normal (97.5th percentile); RVEDVi, right ventricular end-diastolic volume index; RVEF, right ventricular ejection fraction; RV GCS, right ventricular global circumferential strain; RV GLS, right ventricular global longitudinal strain; RV GAS, right ventricular global area strain; REF, radial ejection fraction; AEF, anteroposterior ejection fraction; LEF, longitudinal ejection fraction.

Table 3 Sex-related differences in 3D RV morphological and functional parameters

	All subjects $n = 1043$	Men $n = 533$	Women $n = 510$	*P*- value
RVEDVi (ml)	76.4 ± 20.2	82.2 ± 21.4	70.5 ± 16.9	**<0.001**
RVEF (%)	55.5 ± 5.8	54.5 ± 5.4	56.5 ± 6.0	**<0.001**
RV GCS	−22.1 ± 4.5	−21.9 ± 4.3	−22.3 ± 4.8	0.175
RV GLS	−19.7 ± 3.7	−19.4 ± 3.5	−20.1 ± 3.9	**0.008**
RV GAS	−38.0 ± 5.2	−37.3 ± 4.8	−38.6 ± 5.6	**<0.001**
REF (%)	29.0 ± 7.0	28.3 ± 6.7	29.7 ± 7.1	**0.001**
REF/RVEF	0.52 ± 0.11	0.52 ± 0.11	0.53 ± 0.11	0.284
AEF (%)	25.4 ± 5.9	24.7 ± 5.7	26.1 ± 6.1	**<0.001**
AEF/RVEF	0.45 ± 0.08	0.45 ± 0.08	0.46 ± 0.08	0.188
LEF (%)	21.6 ± 5.7	21.0 ± 5.2	22.3 ± 6.0	**<0.001**
LEF/RVEF	0.39 ± 0.09	0.38 ± 0.08	0.39 ± 0.09	0.144

Statistically significant *P*-values are shown in bold characters.
Ml, millilitres; RVEDVi, right ventricular end-diastolic volume index; RVEF, right ventricular ejection fraction; RV GCS, right ventricular global circumferential strain; RV GLS, right ventricular global longitudinal strain; RV GAS, right ventricular global area strain; REF, radial ejection fraction; AEF, anteroposterior ejection fraction; LEF, longitudinal ejection fraction.

Discussion

The main findings of this study are as follows: (i) smaller RVEDVi and higher RVEF values, with significantly higher GLS and GAS contributions in women compared with men; (ii) significant decrease in global RVEF in older subjects of both sexes, mainly driven by a reduction in the longitudinal component of contraction; (iii) only in women, this reduction of RVEF with increasing age is partially compensated by an increase in REF; and (iv) while black subjects have significantly higher radial and lower longitudinal contributions to global RVEF, white men have higher values of longitudinal and anteroposterior components.

Table 4 Age-related differences in 3D RV morphological and functional parameters

	Men ($n = 533$)				Women ($n = 510$)			
	18–40 years $n = 234$	41–65 years $n = 194$	>65 years $n = 105$	*P*-ANOVA	18–40 years $n = 199$	41–65 years $n = 197$	>65 years $n = 114$	*P*-ANOVA
RVEDVi (ml)	83.4 ± 19.4	80.6 ± 21.9	82.3 ± 24.3	0.364	71.1 ± 17.0	70.0 ± 16.5	70.0 ± 17.3	0.783
RVEF (%)	54.7 ± 5.5	54.7 ± 5.4	53.5 ± 5.1	0.094	56.9 ± 5.9***	57.1 ± 5.9***	55.0 ± 6.1 *,**	**0.005**
RV GCS	−22.0 ± 4.4	−22.0 ± 4.6	−21.8 ± 3.5	0.914	−22.4 ± 5.0	−22.5 ± 4.7	−21.8 ± 4.6	0.281
RV GLS	−20.0 ± 3.4***	−19.5 ± 3.6***	−18.2 ± 3.4*,**	**<0.001**	−20.9 ± 3.9**,***	−20.1 ± 3.8*,***	−18.6 ± 3.7*,**	**<0.001**
RV GAS	−37.7 ± 4.8***	−37.6 ± 4.9***	−36.0 ± 4.2*,**	**0.008**	−39.4 ± 5.6***	−38.9 ± 5.4***	−36.8 ± 5.5*,**	**<0.001**
REF (%)	28.1 ± 6.8	28.5 ± 7.0	28.6 ± 6.3	0.724	28.7 ± 7.2**,***	30.5 ± 7.2*	30.4 ± 6.6*	**0.021**
REF/RVEF	0.51 ± 0.11	0.52 ± 0.11	0.53 ± 0.10	0.233	0.50 ± 0.11**,***	0.53 ± 0.11*	0.55 ± 0.1*	**<0.001**
AEF (%)	24.6 ± 5.6	25.0 ± 5.8	24.4 ± 5.6	0.690	26.3 ± 6.2	26.5 ± 5.9	25.0 ± 6.2	0.098
AEF/RVEF	0.45 ± 0.1	0.45 ± 0.09	0.45 ± 0.1	0.699	0.46 ± 0.09	0.46 ± 0.1	0.45 ± 0.1	0.668
LEF (%)	21.8 ± 5.1***	21.2 ± 5.3***	18.9 ± 4.9*,**	**<0.001**	23.5 ± 6.1***	22.5 ± 5.5***	19.8 ± 6.1*,**	**<0.001**
LEF/RVEF	0.40 ± 0.1***	0.39 ± 0.1***	0.35 ± 0.1*,**	**<0.001**	0.41 ± 0.09**,***	0.39 ± 0.1*,***	0.36 ± 0.1*,**	**<0.001**

Statistically significant *P*-values are shown in bold characters.
Y ,years; ml, millilitres; ANOVA, analysis of variance; RVEDVi, right ventricular end-diastolic volume index; RVEF, right ventricular ejection fraction; RV GCS, right ventricular global circumferential strain; RV GLS, right ventricular global longitudinal strain; RV GAS, right ventricular global area strain; REF, radial ejection fraction; AEF, anteroposterior ejection fraction; LEF, longitudinal ejection fraction.
*$P < 0.05$ vs. 18–40-year age group.
**$P < 0.05$ vs. 41–65-year age group.
***$P < 0.05$ vs. >65 years age group.

Table 5 Race-related differences in 3D RV morphological and functional parameters

	Men ($n = 510$)				Women ($n = 495$)			
	White $n = 235$	Black $n = 69$	Asian $n = 206$	*P*-ANOVA	White $n = 253$	Black $n = 73$	Asian $n = 169$	*P*-ANOVA
RVEDVi (ml)	85.7 ± 21.6**,***	95.5 ± 23.7*,***	74.4 ± 17*,**	**<0.001**	70.9 ± 16.7*,**	81.2 ± 16.8*,***	65.7 ± 16*,**	**<0.001**
RVEF (%)	55.4 ± 5.9**,***	52.4 ± 4.5*,***	54.2 ± 5.0*,**	**<0.001**	57.2 ± 6.1**	54.9 ± 5.1*	56.2 ± 6.1	**0.010**
RV GCS	−22.4 ± 4.4***	−21.4 ± 4.1	−21.5 ± 4.2*	**0.034**	−22.5 ± 4.7	−22.1 ± 4.6	−22.1 ± 5.1	0.627
RV GLS	−20.2 ± 3.5**,***	−18.2 ± 3.3*	−19.1 ± 3.5*	**<0.001**	−20.1 ± 4.0	−19.2 ± 3.8	−20.3 ± 3.9	0.119
RV GAS	−38.3 ± 5.0**,***	−35.2 ± 4.2*,***	−37.0 ± 4.5*,**	**<0.001**	−38.7 ± 5.6**	−37.1 ± 5.0*,***	−39.0 ± 5.8**	**0.036**
REF (%)	28.1 ± 7.1	29.1 ± 5.7	28.3 ± 6.7	0.598	30.3 ± 7.5	29.3 ± 6.4	29.3 ± 7.0	0.261
REF/RVEF	0.50 ± 0.11**	0.55 ± 0.09*,***	0.52 ± 0.11**	**0.004**	0.53 ± 0.11	0.53 ± 0.10	0.52 ± 0.11	0.656
AEF (%)	25.5 ± 5.8**	22.5 ± 4.9*,***	24.6 ± 5.7**	**0.001**	26.3 ± 6.1	24.9 ± 4.8	26.2 ± 6.7	0.221
AEF/RVEF	0.46 ± 0.08**	0.43 ± 0.08*	0.45 ± 0.9	**0.046**	0.46 ± 0.08	0.45 ± 0.07	0.46 ± 0.09	0.706
LEF (%)	22.3 ± 5.2**,***	18.0 ± 4.8*,***	20.6 ± 4.9*,**	**<0.001**	22.8 ± 6.1**	20.3 ± 5.7*,***	22.3 ± 6.1**	**0.011**
LEF/RVEF	0.40 ± 0.08**,***	0.34 ± 0.08*,***	0.38 ± 0.1*,**	**<0.001**	0.40 ± 0.09	0.37 ± 0.09	0.39 ± 0.09	0.087

Statistically significant *P*-values are shown in bold characters.
Ml, millilitres; ANOVA, analysis of variance; RVEDVi, right ventricular end-diastolic volume index; RVEF, right ventricular ejection fraction; RV GCS, right ventricular global circumferential strain; RV GLS, right ventricular global longitudinal strain; RV GAS, right ventricular global area strain; REF, radial ejection fraction; AEF, anteroposterior ejection fraction; LEF, longitudinal ejection fraction.
*$P < 0.05$ vs. 18–40-year age group.
**$P < 0.05$ vs. 41–65-year age group.
***$P < 0.05$ vs. >65 years age group.

Rationale for the evaluation of non-longitudinal components of RV contraction

The RV myo-architecture and contraction are extremely complex. While the septum is characterized by oblique longitudinal and spiral fibres, the RV free wall contains predominantly transversal myofibres.[14] Due to this unique spatial anatomical disposition of myofibres, RV contraction is the result of the combination of three distinctive contractile patterns i.e. shortening along the longitudinal axis, radial contraction of the free wall ('bellows effect'), and anteroposterior shortening as a result of LV contraction.

However, all 2DE techniques used for the evaluation of RV contraction provide information on regional, rather than global RV function. 2DE RV FWS has the advantage of being a more sensitive indicator of subclinical impairment of RV contraction than conventional 2DE measurements.[2,15,16] Nevertheless, it has been reported that in situations where RV function is not predominantly affected by reduced longitudinal contraction or where global RV function remains preserved despite decreased longitudinal motion, the sole use of 2DE RV FWS might be insufficient to characterize RV systolic function.[17,18]

3DE assessment of RV volumes, EF, and GLS are feasible and reproducible[19] and provide additional prognostic information in diverse cardiac conditions.[20,21] Moreover, constant advances and development of matrix-array transducers with higher spatial and temporal resolutions made possible the development of dedicated software for 3DE deconstruction of RV contraction into its motion components. The software used in our study has previously shown excellent intra- and inter-observer reproducibility as well as a robust correlation with currently available echocardiographic software and a modest correlation with CMR,[11,22] mainly explained by the single centre, and observational characteristics of the studies where these correlations were evaluated.

Evidence about the clinical utility of the different components of RV systolic function

The prognostic value of the parameters included in our study has been described by Kitano *et al.*[22], who showed that 3D RV GCS, GLS, and GAS were associated with cardiac death, ventricular tachyarrhythmia, or heart failure hospitalization in patients with diverse cardiac diseases. Moreover, these findings persisted after adjusting for factors like age, renal function, LVEF, and average mitral E/e′. Kaplan–Meier analysis showed that median values of 3D RV GCS, GLS, and GAS accurately stratified these patients by survival rates.[22] Interestingly, 3D RV GAS was shown to be a better prognosticator than RV GLS or GCS, most likely due to the fact that the information provided by GAS corresponds to a multiplanar evaluation of RV contraction and is not limited to either longitudinal or circumferential motion.[22] Tolvaj *et al.*[23] have described the association between reduced RV GCS and increased risk of all-cause mortality, even in scenarios where LV GLS is preserved. Importantly, it is paramount to understand that the RV adaptive mechanisms vary according to the underlying pathophysiological process, and therefore, such detailed assessment has allowed the identification of distinctive RV mechanical adaptations in different populations,[22,24–26] including heart transplant recipients,[27] congenital cardiomyopathies,[28] and elite athletes.[29]

In patients with mildly and moderately reduced LVEF, Surkova *et al.* demonstrated that despite initially reduced LEF and AEF, REF increased, thus maintaining global RV performance. Once the contribution of REF decreased, global RVEF became severely reduced.[30] In patients with preserved RVEF (>45%), the AEF component has shown to be a significant and independent predictor of outcome after a median of 6.7 years follow-up.[30] Moreover, in a meta-analysis of more than 1900 patients, Sayour *et al.*[31] have demonstrated that 3D RVEF has a stronger association with adverse cardiopulmonary outcomes than conventional 2DE RV functional indices, namely TAPSE, FAC, and RV FWS. These findings question the clinical usefulness of those conventional RV functional parameters that refer exclusively to longitudinal shortening and highlight the importance of a multiparametric or 3D-based assessment. Detecting the functional decrease at other motion directions could aid to identify early dysfunction markers in specific disease states and may support a better monitoring and therapeutic decision making.

Timely diagnosis and appropriate risk stratification of patients with severe mitral regurgitation (MR) represent a major clinical need.[32] Interestingly, Tokodi *et al.* reported that in patients with severe primary MR and RVEF > 45%, there was an initial reduction in REF and a predominant contribution of LEF to the global RV contraction. However, in the immediate post-operative period, this contractile RV pattern inverted, and REF prevailed over LEF. Interestingly, after 6 months, the contribution of both components had equalized.[25]

These reports reinforce the notion that the impact of ventricular interdependence and the different haemodynamic conditions on RV systolic function might be overlooked, if the evaluation of RV contraction is only performed using conventional parameters of longitudinal shortening. The question whether these changes in RV contraction patterns might be useful as surrogates of early RV dysfunction and represent additional criteria for intervention will require further prospective research in patients with specific pathologies.

Contributions of the current study

Although Lakatos *et al.* have previously described the contribution of non-longitudinal components of RV contraction,[12] our study broadens this analysis to the larger, multicentric, and multiethnic WASE cohort, yielding a more statistically sound assessment of the influence of sex, age, and race on these parameters. The LLN and ULN values for 3D RVEDVi and RVEF provided by our study are similar to those reported by the two largest studies of 3DE normative values of this chamber.[33,34]

Current clinical practice lacks RV functional parameters that represent the non-longitudinal shortening of this chamber. The results of our study expand the evidence provided by previous reports, showing that REF and AEF have similar contributions to that of LEF to global RV contraction, and that these components should not be neglected when evaluating RV function.[12] We showed that RV contraction pattern is independently associated with age, sex, and race, highlighting that the established changes across the different subgroups are not just due to anthropometric or basic haemodynamic differences. The magnitudes of longitudinal and anteroposterior shortening are coupled with LV function; however, radial shortening is not. This observation is in line with the findings of Surkova *et al.*[30] who showed that these mechanical directions deteriorate in parallel with LV systolic dysfunction.

Our findings agree with those reported in the 2D RV systolic function analysis on the WASE population, which have shown that RV dimensions were larger in men and 2D RV functional parameters were larger in women.[35] Age-related changes in these 2D parameters were not uniform,[35] and previous studies using 3DE assessment of RV systolic function have also noted that age is weakly correlated with RVEF.[33] Notably, we were able to identify an age-related reduction in the longitudinal components of RV contraction in both sexes and a characteristic increase in radial RV contraction in women with age. These observations might be related to an age-related increase in pulmonary pressures and consequent changes in RV myofibre architecture. A preserved RVEF does not preclude changes in individual RV contractile components, and the role of REF as an early marker of elevated pulmonary pressures has already been proposed.[17] Muraru *et al.*[36] have identified LV GLS and pulmonary pressures as independent predictors of RV longitudinal performance, suggesting that the

assessment of the RV adaptation to increased afterload should not be limited to the RV free wall. Accordingly, our findings emphasize that the evaluation of RV systolic function in individuals > 65 years should not be restricted to its longitudinal motion.

Although noticeable differences in 3D RV volumes and EF across ethnic groups have been recently identified,[34] to our knowledge, this is the first study describing distinctive RV contractile patterns in black and white men, which had been previously overlooked when only using 2DE parameters.[35]

Limitations

The feasibility of 3D RV analysis in the WASE cohort was slightly above 50%.[34] It must be acknowledged that 3DE acquisitions of the right ventricle are technically demanding, requiring a high level of expertise. Low accuracy of automated measurements in right ventricles of different geometry and image quality should also be considered.[37,38] Furthermore, in our study, there was a relative under-representation of black subjects and individuals from the older age group.

Conclusion

Mechanical adaptations of the right ventricle are complex and are often not restricted to its longitudinal motion. The clinical and prognostic utility of the different components of 3DE RV function has been previously reported. Our results expand the evidence on physiological contributions of longitudinal and non-longitudinal RV contraction and the presence of sex-, age-, and race-related differences in these components. These findings might be useful in considering both physiological and pathological states involving the right ventricle.

Supplementary data

Supplementary data are available at *European Heart Journal - Cardiovascular Imaging* online.

Conflict of interest: A.K. serves as the Chief Medical Officer of Argus Cognitive, Inc. and received financial compensation for his work, outside the submitted paper. No direct conflicts of interest related to this study have been reported by other authors. All authors have been involved in the design of the WASE study, patient enrolment, and/or data analysis, and all have critically reviewed and approved the final manuscript prior to submission. A full list of WASE investigators is provided in the footnote.

Data availability

Data used in this study will not be publicly available.

References

1. Antoni ML, Scherptong RWC, Atary JZ, Boersma E, Holman ER, van der Wall EE *et al.* Prognostic value of right ventricular function in patients after acute myocardial infarction treated with primary percutaneous coronary intervention. *Circ Cardiovasc Imaging* 2010;**3**:264–71.
2. Carluccio E, Biagioli P, Alunni G, Murrone A, Zuchi C, Coiro S *et al.* Prognostic value of right ventricular dysfunction in heart failure with reduced ejection fraction: superiority of longitudinal strain over tricuspid annular plane systolic excursion. *Circ Cardiovasc Imaging* 2018;**11**:e006894.
3. Amsallem M, Sweatt AJ, Aymami MC, Kuznetsova T, Selej M, Lu H *et al.* Right heart end-systolic remodeling index strongly predicts outcomes in pulmonary arterial hypertension: comparison with validated models. *Circ Cardiovasc Imaging* 2017;**10**:e005771.
4. Spiewak M, Małek LA, Petryka J, Mazurkiewicz L, Werys K, Biernacka EK *et al.* Repaired tetralogy of Fallot: ratio of right ventricular volume to left ventricular volume as a marker of right ventricular dilatation. *Radiology* 2012;**265**:78–86.
5. Ho SY, Nihoyannopoulos P. Anatomy, echocardiography, and normal right ventricular dimensions. *Heart* 2006;**92**(Suppl 1):i2–13.
6. Lakatos B, Toser Z, Tokodi M, Doronina A, Kosztin A, Muraru D *et al.* Quantification of the relative contribution of the different right ventricular wall motion components to right ventricular ejection fraction: the ReVISION method. *Cardiovasc Ultrasound* 2017;**15**:8.
7. Asch FM, Banchs J, Price R, Rigolin V, Thomas JD, Weissman NJ *et al.* Need for a global definition of normative echo values-rationale and design of the World Alliance of Societies of Echocardiography Normal Values Study (WASE). *J Am Soc Echocardiogr* 2019;**32**:157–162 e2.
8. Asch FM, Miyoshi T, Addetia K, Citro R, Daimon M, Desale S *et al.* Similarities and differences in left ventricular size and function among races and nationalities: results of the World Alliance Societies of Echocardiography Normal Values Study. *J Am Soc Echocardiogr* 2019;**32**:1396–1406 e2.
9. Lang RM, Badano LP, Mor-Avi V, Afilalo J, Armstrong A, Ernande L *et al.* Recommendations for cardiac chamber quantification by echocardiography in adults: an update from the American society of Echocardiography and the European Association of Cardiovascular Imaging. *J Am Soc Echocardiogr* 2015;**28**:1–39 e14.
10. Medvedofsky D, Addetia K, Patel AR, Sedlmeier A, Baumann R, Mor-Avi V *et al.* Novel approach to three-dimensional echocardiographic quantification of right ventricular volumes and function from focused views. *J Am Soc Echocardiogr* 2015;**28**:1222–31.
11. Tokodi M, Staub L, Budai A, Lakatos BK, Csakvari M, Suhai FI *et al.* Partitioning the right ventricle into 15 segments and decomposing its motion using 3D echocardiography-based models: the updated ReVISION method. *Front Cardiovasc Med* 2021;**8**:622118.
12. Lakatos BK, Nabeshima Y, Tokodi M, Nagata Y, Tősér Z, Otani K *et al.* Importance of nonlongitudinal motion components in right ventricular function: three-dimensional echocardiographic study in healthy volunteers. *J Am Soc Echocardiogr* 2020;**33**:995–1005 e1.
13. Addetia K, Miyoshi T, Amuthan V, Citro R, Daimon M, Gutierrez Fajardo P *et al.* Normal values of left ventricular size and function on three-dimensional echocardiography: results of the World Alliance Societies of Echocardiography study. *J Am Soc Echocardiogr* 2022;**35**:449–59.
14. Buckberg G, Mahajan A, Saleh S, Hoffman JI, Coghlan C. Structure and function relationships of the helical ventricular myocardial band. *J Thorac Cardiovasc Surg* 2008;**136**:578–89. 589 e1–11.
15. Muraru D, Haugaa K, Donal E, Stankovic I, Voigt JU, Petersen SE *et al.* Right ventricular longitudinal strain in the clinical routine: a state-of-the-art review. *Eur Heart J Cardiovasc Imaging* 2022;**23**:898–912.
16. D'Andrea A, Limongelli G, Baldini L, Verrengia M, Carbone A, Di Palma E *et al.* Exercise speckle-tracking strain imaging demonstrates impaired right ventricular contractile reserve in hypertrophic cardiomyopathy. *Int J Cardiol* 2017;**227**:209–16.
17. Kind T, Mauritz GJ, Marcus JT, van de Veerdonk M, Westerhof N, Vonk-Noordegraaf A. Right ventricular ejection fraction is better reflected by transverse rather than longitudinal wall motion in pulmonary hypertension. *J Cardiovasc Magn Reson* 2010;**12**:35.
18. Tamborini G, Muratori M, Brusoni D, Celeste F, Maffessanti F, Caiani EG *et al.* Is right ventricular systolic function reduced after cardiac surgery? A two- and three-dimensional echocardiographic study. *Eur J Echocardiogr* 2009;**10**:630–4.
19. Li Y, Zhang L, Gao Y, Wan X, Xiao Q, Zhang Y *et al.* Comprehensive assessment of right ventricular function by three-dimensional speckle-tracking echocardiography: comparisons with cardiac magnetic resonance imaging. *J Am Soc Echocardiogr* 2021;**34**:472–82.
20. Nagata Y, Wu VC, Kado Y, Otani K, Lin FC, Otsuji Y *et al.* Prognostic value of right ventricular ejection fraction assessed by transthoracic 3D echocardiography. *Circ Cardiovasc Imaging* 2017;**10**:e005384.
21. Muraru D, Badano LP, Nagata Y, Surkova E, Nabeshima Y, Genovese D *et al.* Development and prognostic validation of partition values to grade right ventricular dysfunction severity using 3D echocardiography. *Eur Heart J Cardiovasc Imaging* 2020;**21**:10–21.
22. Kitano T, Kovacs A, Nabeshima Y, Tokodi M, Fabian A, Lakatos BK *et al.* Prognostic value of right ventricular strains using novel three-dimensional analytical software in patients with cardiac disease. *Front Cardiovasc Med* 2022;**9**:837584.
23. Tolvaj M, Fábián A, Tokodi M, Lakatos B, Assabiny A, Ladanyi Z *et al.* There is more than just longitudinal strain: prognostic significance of biventricular circumferential mechanics. *Front Cardiovasc Med* 2023;**10**:1082725.
24. Moceri P, Duchateau N, Gillon S, Jaunay L, Baudouy D, Squara F *et al.* Three-dimensional right ventricular shape and strain in congenital heart disease patients with right ventricular chronic volume loading. *Eur Heart J Cardiovasc Imaging* 2021;**22**:1174–81.
25. Tokodi M, Németh E, Lakatos BK, Kispál E, Tősér Z, Staub L *et al.* Right ventricular mechanical pattern in patients undergoing mitral valve surgery: a predictor of postoperative dysfunction? *ESC Heart Fail* 2020;**7**:1246–56.
26. Kovács A, Lakatos B, Tokodi M, Merkely B. Right ventricular mechanical pattern in health and disease: beyond longitudinal shortening. *Heart Fail Rev* 2019;**24**:511–20.
27. Lakatos BK, Tokodi M, Assabiny A, Tősér Z, Kosztin A, Doronina A *et al.* Dominance of free wall radial motion in global right ventricular function of heart transplant recipients. *Clin Transplant* 2018;**32**:e13192.
28. Surkova E, Kovács A, Lakatos BK, Tokodi M, Fábián A, West C *et al.* Contraction patterns of the systemic right ventricle: a three-dimensional echocardiography study. *Eur Heart J Cardiovasc Imaging* 2022;**23**:1654–62.

29. Fábián A, Ujvári A, Tokodi M, Lakatos BK, Kiss O, Babity M *et al.* Biventricular mechanical pattern of the athlete's heart: comprehensive characterization using three-dimensional echocardiography. *Eur J Prev Cardiol* 2022;**29**:1594–604.
30. Surkova E, Kovács A, Tokodi M, Lakatos BK, Merkely B, Muraru D *et al.* Contraction patterns of the right ventricle associated with different degrees of left ventricular systolic dysfunction. *Circ Cardiovasc Imaging* 2021;**14**:e012774.
31. Sayour AA, Tokodi M, Celeng C, Takx RAP, Fabian A, Lakatos BK *et al.* Association of right ventricular functional parameters with adverse cardiopulmonary outcomes: a meta-analysis. *J Am Soc Echocardiogr* 2023;**36**:624–633.e8.
32. Baumgartner H, Falk V, Bax JJ, De Bonis M, Hamm C, Holm PJ *et al.* 2017 ESC/EACTS guidelines for the management of valvular heart disease. *Eur Heart J* 2017;**38**:2739–91.
33. Maffessanti F, Muraru D, Esposito R, Gripari P, Ermacora D, Santoro C *et al.* Age-, body size-, and sex-specific reference values for right ventricular volumes and ejection fraction by three-dimensional echocardiography: a multicenter echocardiographic study in 507 healthy volunteers. *Circ Cardiovasc Imaging* 2013;**6**:700–10.
34. Addetia K, Miyoshi T, Amuthan V, Citro R, Daimon M, Gutierrez Fajardo P *et al.* Normal values of 3D right ventricular size and function measurements: results of the World Alliance of Societies of Echocardiography study. *J Am Soc Echocardiogr* 2023;**36**:858–866.e1.
35. Addetia K, Miyoshi T, Citro R, Daimon M, Gutierrez Fajardo P, Kasliwal RR *et al.* Two-dimensional echocardiographic right ventricular size and systolic function measurements stratified by sex, age, and ethnicity: results of the World Alliance of Societies of Echocardiography study. *J Am Soc Echocardiogr* 2021;**34**:1148–1157 e1.
36. Muraru D, Onciul S, Peluso D, Soriani N, Cucchini U, Aruta P *et al.* Sex- and method-specific reference values for right ventricular strain by 2-dimensional speckle-tracking echocardiography. *Circ Cardiovasc Imaging* 2016;**9**:e003866.
37. Ostenfeld E, Carlsson M, Shahgaldi K, Roijer A, Holm J. Manual correction of semi-automatic three-dimensional echocardiography is needed for right ventricular assessment in adults; validation with cardiac magnetic resonance. *Cardiovasc Ultrasound* 2012;**10**:1.
38. Muraru D, Badano LP, Piccoli G, Gianfagna P, Del Mestre L, Ermacora D *et al.* Validation of a novel automated border-detection algorithm for rapid and accurate quantitation of left ventricular volumes based on three-dimensional echocardiography. *Eur J Echocardiogr* 2010;**11**:359–68.